

X-BAND LINEAR COLLIDER R&D IN ACCELERATING STRUCTURES THROUGH ADVANCED COMPUTING*

Zenghai Li, Nathan T. Folwell, Lixin Ge, Adam Guetz, Valentin Ivanov, Marc Kowalski, Lie-Quan Lee, Cho-Kuen Ng, Greg Schussman, Ravindra Uplenchwar, Michael Wolf¹, and Kwok Ko, SLAC, ¹University of Illinois, Urbana-Champaign, USA

Abstract

This paper describes a major computational effort that addresses key design issues in the high gradient accelerating structures for the proposed X-band linear collider, GLC/NLC. Supported by the US DOE's Accelerator Simulation Project, SLAC is developing a suite of parallel electromagnetic codes based on unstructured grids for modeling RF structures with higher accuracy and on a scale previously not possible. The new simulation tools have played an important role in the R&D of X-Band accelerating structures, in cell design, wakefield analysis and dark current studies.

INTRODUCTION

The X-band linear collider design, GLC/NLC [1], requires accelerating structures in the main linac to operate at 65 MV/m, and to be able to control emittance growth due to dipole wakefields generated by 100 micron bunches. In addition, the tolerance on the accelerating cell needs to be micron level to maintain maximum efficiency. The path to high gradient has focused on testing structures for acceptable breakdown rates at the desired gradient through experiments as theoretical approaches are challenging. The damped, detuned structure (DDS) has shown capable of suppressing dipole wakefields to meet design requirements but the analysis using equivalent circuits has been limited to the first two dipole-bands. And modeling the 3D DDS cell geometry to micron level accuracy is beyond the capability of existing codes.

The present work represents a new modeling approach that combines unstructured grids with parallel computing to achieve the required accuracy and scale of simulation. The parallel electromagnetic field solvers developed at SLAC under the US DOE's SciDAC [2] Accelerator Simulation Project include the eigensolver **Omega3P**, S-parameter solver **S3P**, time domain solver **T3P**, all of which are based on finite element formulation on tetrahedral meshes, plus another time domain solver **Tau3P** which uses generalized Yee hexahedral meshes. A tracking module **Track3P** has also been developed for dark current simulation involving both primary and secondary emissions. Numerical results from application of these codes to the X-band accelerating structure R&D are presented in the following three sections.

DDS CELL DESIGN

The Damped, Detuned Structure (DDS) for the NLC main linac is a fully 3D design that is optimized for higher shunt impedance (14% increase over existing design) and incorporates wakefield suppression through Gaussian detuning and manifold damping. The challenge was to model the complex geometry (Fig. 1) to accuracies close to machining tolerance, requiring an eigensolver that can calculate resonant frequencies accurate to 0.01%.

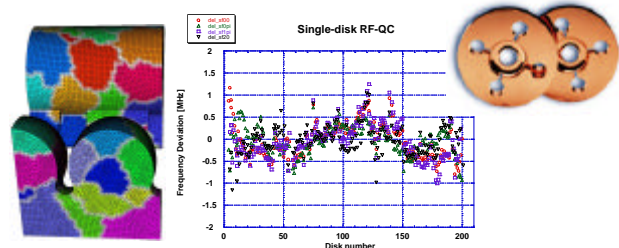


Figure 1: (Left) A distributed Omega3P model of 1/8 of the DDS, (right) microwave QC of the fabricated cells (insert) showing measured data within 0.01% of target frequency.

Using Omega3P on the massively parallel computers at NERSC, a table of dimensions for cells along a DDS section was generated for computerized machining based on calculations that met the 0.01% frequency criteria. Microwave QCs on fabricated cells showed that their measured frequencies are indeed within 1 MHz of the target value of 11.424 GHz. This result demonstrates that **high resolution modeling** together with high precision machining can provide the capability for designing and manufacturing the DDS cells for the X-band collider.

DDS WAKEFIELD ANALYSIS

The present baseline design for the X-band collider is the H60VG4 [3](Fig. 2) which is a 55-cell DDS structure in which the dimensions of the cells are chosen such that the dipole modes are detuned in a Gaussian manner for the wakefields to decohere and be reduced along the bunch train. The cells are connected via slot openings to four vacuum manifolds that function also as damping conduits for the dipole wakefields to be taken out and absorbed in matched loads. The wakefields have been calculated using an equivalent circuit model that only includes the contributions of the first two dipole bands. We have modeled the entire 55-cell structure with exact dimension both in the time and frequency domain. The

* Work supported by the U.S. DOE Contract No. DE-AC03-76SF00515.

end-to-end simulations were carried out with **Tau3P** and **Omega3P** respectively using the IBM/SP3 computer at NERSC.



Figure 2: Model of the H60VG4 DDS structure with damping manifolds, input/output power couplers and HOM couplers.

Time-domain Simulation Using **Tau3P**, the H60VG4 has been simulated for the first time with a transit beam so that the complete wakefield was found directly. Figure 3 shows the beam-excited electric fields in the structure at two instances in time. Figure 4 compares the impedance spectrum and the wakefields between the DDS in red and the DS (Detuned Structure without the manifold) in blue, clearly showing the dramatic manifold damping effect on the long range wakefields.

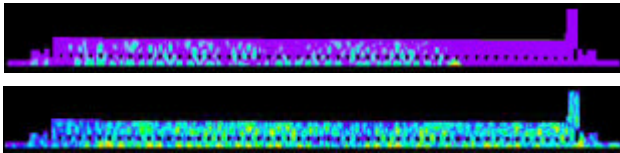


Figure 3: Beam excited electric fields in the H60VG4 at two instances in time as modeled by Tau3P.

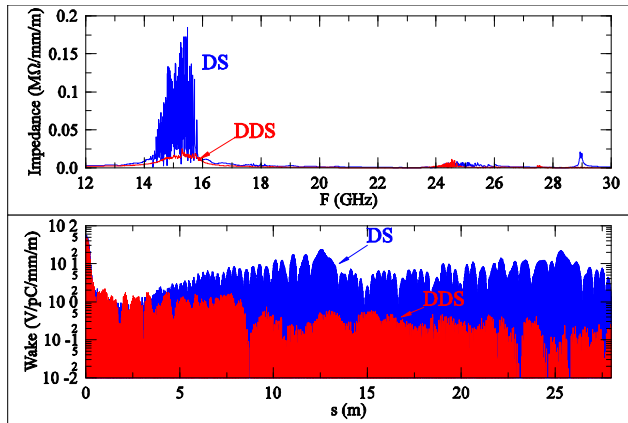


Figure 4: (Top) Impedance spectrum of DDS (red) and DS (blue), and (bottom) wakefields in DDS (red) and DS (blue) all from Tau3P simulations.

Frequency-domain Calculation A complex solver has been implemented in Omega3P for finding damped modes in cavities with lossy materials. It was applied to the H60VG4 structure in which all waveguide openings were terminated in external matched loads. Modes up to the 3rd band have been calculated (Fig. 5) and for 120 eigen-pairs the simulation took 3179 seconds using 512 processors on the IBM/SP3 to solve a matrix system with 94.5 million non-zeros, representing a DDS quadratic element model of 2.3 million degrees of freedom. The eignmodes in the 1st band belong to two groups, those with relatively low kick factor/high Q and couple to the upstream end of the manifold (Fig. 6), suggesting HOM loads are needed in the input end, and those with high kick factor/ low Q that

couple downstream to the manifold to terminate in the HOM loads (Fig. 6),

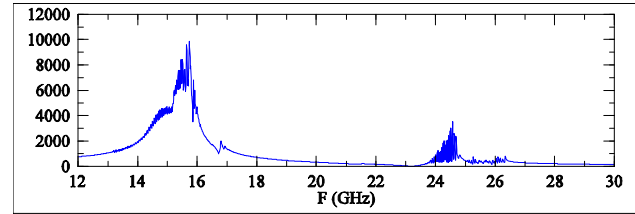


Figure 5: Impedance spectrum of H60VG4 up to 3rd band from Omega3P calculations. .

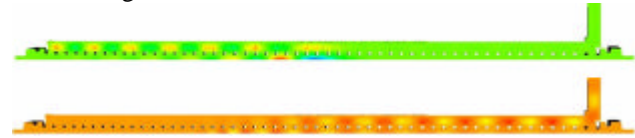


Figure 6: (Top) Eigenmode with low kick factor/high Q from Omega3P in 1st band of the H60VG4, and (bottom) eigenmode with high kick factor/low Q in same structure.

Wakefield Comparison The simulations with **Omega3P** and **Tau3P** were the first ever modeling of an entire DDS prototype as built, and provided direct verification of the combined damping and detuning wakefield suppression scheme. Figure 7 compares the wakefields from **Omega3P** and **Tau3P** which show excellent agreement.

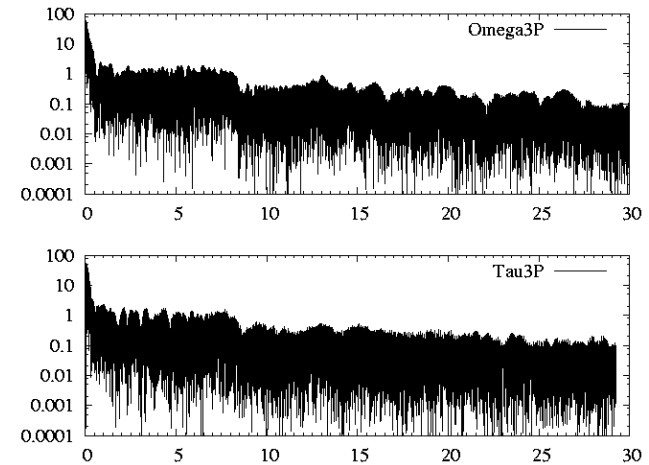


Figure 7: (Top) Wakefields in H60VG4 from Omega3P frequency-domain calculation, and (bottom) wakefields in same structure from Tau3P time-domain simulation.

DARK CURRENT SIMULATION

Dark current could limit a linac from operating at a higher field gradient. At high fields, primary electrons are generated by field emission which further generate secondary electrons upon impact with the wall surface. Electrons that are captured by the accelerating field form the dark current which can perturb the main beam and interfere with the data analysis at the IP. It is also known to be the precursor to RF breakdown. As part of SciDAC, the parallel tracking code **Track3P** is under development aimed at building an accurate, quantitative model of the dark current generation and capture. It uses the fields generated by the parallel field solvers **Omega3P** for

standing wave cavities, and *Tau3P/T3P* for traveling wave structures. A surface physics module that contains models for field emission and secondary emission processes has been implemented. Benchmarking has been done on a square waveguide bend (Fig. 8) for which high power test data are available and good agreement is found on the X-ray spectrum generated.

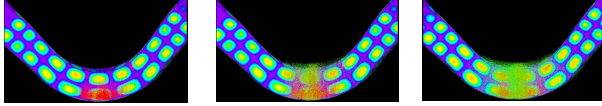


Figure 8: Evolution to steady state of surface emissions in NLC square waveguide bend at high power. Wave travels from left to right. Primary particles are red and secondaries are green.

High power test data are also available on a 30-cell X-band constant impedance structure for which the downstream dark current has been measured for drive pulses with different risetimes and at different field gradients. Pulse risetime results in dispersive effects that lead to peak field enhancements in the structure due to overshoot with shorter risetime producing larger field enhancement as demonstrated by *Tau3P* simulations (Fig. 9).

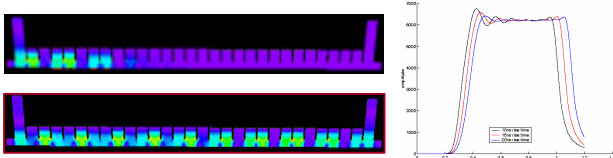


Figure 9: (Left) Snapshots of pulse propagation using *Tau3P* in 30-cell constant impedance structure, and (right) field enhancements due to 10 nsec (black), 15 nsec (red), and 20 nsec (blue) pulse risetime monitored at the disk of a cell near the output end.

Using the fields calculated with *Tau3P*, the dark current in the 30-cell structure has been simulated with *Track3P* for three different risetimes, 10, 15 and 20 nsec and field gradients of 65 and 85 MV/m. A beta of 40 was used in the Fowler-Nordheim field emission model. Figure 10 shows a sequence of time plots that capture the dark current generation as the drive pulse propagates through the structure via the input/output couplers. Field emitted particles in red emerged from the cell disks where the fields are the highest. Secondaries in green were generated later in time. The dark current downstream was monitored and the results for the three different risetimes of the drive pulse are plotted in Fig. 11. The dark current pulse shapes bear resemblance to the respective field enhancement at the cell disk for the same drive pulse (Fig. 9), indicating that dispersive effects play an important role in dark current generation. The dark current pulses are compared with measurement [4] (Fig. 11) and reasonable agreement is found. Work is in progress to perform the same numerical studies on the H60VG4 which is a more computationally intensive endeavor because it is a much larger and more complicated structure.

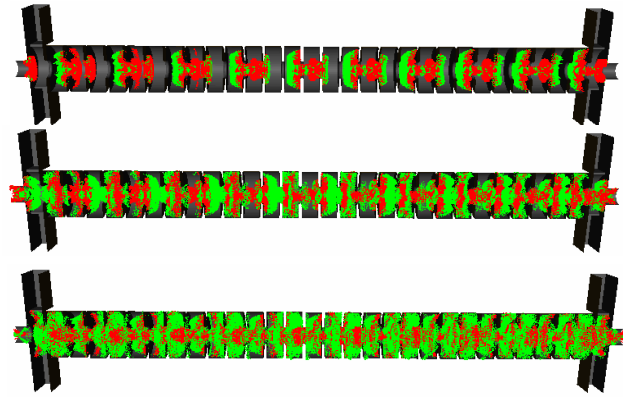


Figure 10: Snapshots of dark current generation in 30-cell structure as simulated with *Track3P* for a realistic drive pulse propagating from left to right. Red particles are primaries while green particles are secondaries.

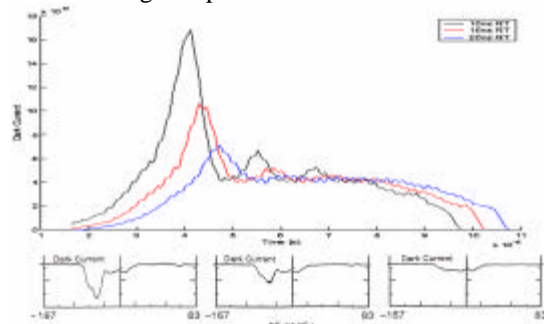


Figure 11: (Top) Dark current pulses calculated in *Track3P* downstream of the 30-cell structure for drive pulses of three different risetimes (black is 10 nsec, red is 15 nsec, and blue is 20 nsec). (Bottom) Downstream dark current pulses from experiment for same three drive pulses in order from left to right, 10 nsec, 15 nsec and 20 nsec, showing good agreement with simulation.

SUMMARY

Advanced computing has enabled electromagnetic modeling to achieve higher resolution and larger problem size than previously possible. Developed under SciDAC, a new suite of parallel tools based on unstructured grids has been applied successively to the design of complex cavities with high accuracy, and to realize end-to-end simulation of accelerator systems. This computational effort has had a significant impact on the accelerating structure R&D for the X-band linear collider.

REFERENCES

- [1] ZDR report for the Next Linear Collider, LBNL-PUB-5424, SLAC Report 474, UCRL-ID-124161, 1996.
- [2] Kwok Ko, et al, Electromagnetic Systems Simulation - "From Simulation to Fabrication", SciDAC Report, 2003.
- [3] Zenghai Li, JLC/NLC X-Band Structure Design, JLC/NLC ISG11, KEK, Japan, December 16-19, 2003.
- [4] J.W. Wang, et al., High Gradient Studies on 11.4-GHz Copper Accelerator Structures, Proc. LINAC 92, p716-718, Ottawa, Canada, Aug. 24-28, 1992.